Age-related Changes in Rat Myocardium Involve Altered Capacities of Glycosaminoglycans to Potentiate Growth Factor Functions and Heparan Sulfate-altered Sulfation*[S]

Minh Bao Huynh[‡1], Christophe Morin[‡], Gilles Carpentier[‡], Stephanie Garcia-Filipe[‡], Sofia Talhas-Perret[‡], Véronique Barbier-Chassefière[‡], Toin H. van Kuppevelt[§], Isabelle Martelly[‡], Patricia Albanese[‡], and Dulce Papy-Garcia[‡2]

From the [‡]Laboratoire Croissance, Reparation et Regeneration Tissulaires EAC/CNRS-7149, Université Paris Est Créteil, 94010 Créteil, France and the [§]Department of Matrix Biochemistry, Nijmegen Centre for Molecular Life Sciences, Radboud University, 6500 HC Nijmegen, The Netherlands.

Background: Heparan sulfates (HS) are important cell behavior regulators.
Results: With age, HS structural changes affect myocardial growth factor functionalities.
Conclusion: This reveals the importance of HS on the control of essential tissue repair effectors during aging.
Significance: Changes in cardiac HS may alter tissue homeostasis and impair heart function. This might also limit the success of protein therapies and implantation of therapeutic cells.

Glycosaminoglycans (GAGs) are essential components of the extracellular matrix, the natural environment from which cell behavior is regulated by a number or tissue homeostasis guarantors including growth factors. Because most heparin-binding growth factor activities are regulated by GAGs, structural and functional alterations of these polysaccharides may consequently affect the integrity of tissues during critical physiological and pathological processes. Here, we investigated whether the aging process can induce changes in the myocardial GAG composition in rats and whether these changes can affect the activities of particular heparin-binding growth factors known to sustain cardiac tissue integrity. Our results showed an age-dependent increase of GAG levels in the left ventricle. Biochemical and immunohistological studies pointed out heparan sulfates (HS) as the GAG species that increased with age. ELISA-based competition assays showed altered capacities of the aged myocardial GAGs to bind FGF-1, FGF-2, and VEGF but not HB EGF. Mitogenic assays in cultured cells showed an age-dependent decrease of the elderly GAG capacities to potentiate FGF-2 whereas the potentiating effect on $VEGF_{165}$ was increased, as confirmed by augmented angiogenic cell proliferation in Matrigel plugs. Moreover, HS disaccharide analysis showed considerably altered 6-O-sulfation with modest changes in N- and 2-O-sulfations. Together, these findings suggest a physiological significance of HS structural and functional alterations during aging. This can be associated with an age-dependent decline of the extracellular matrix capacity to efficiently modulate not only the activity of resident or therapeutic growth factors but also the homing of resident or therapeutic cells.

For many years, it has become clear that the extracellular matrix (ECM)[3] plays complex and divergent roles influencing cell behavior and maintaining tissue homeostasis (1). Alterations of the ECM components as a consequence of pathology, tissue injury, or aging might thus affect tissue integrity and influence the decline of vulnerable organs, such as heart (2). For many years, it has been established that, as age advances, the ability of myocardium to resist to injury declines markedly, making of aging the major risk factor for heart failure.

Proteoglycans and their glycosaminoglycan (GAG) moieties are among the major EMC components known to support, protect, and trigger the activity of informative molecules, including growth factors, cytokines, and other guarantors of tissue homeostasis (3). GAGs are long anionic polysaccharides formed of particular disaccharide building blocks that differentiate hyaluronan, heparan sulfates (HS), chondroitin sulfates, and keratan sulfates subfamilies. HS are characterized by a high structural complexity related to a large variety of sulfation patterns present along the polysaccharide chains (4). It is now accepted that particular sulfated sequences can interact specifically with growth factors and cytokines for which GAGs have being identified as essential low affinity receptors (5). Hence, structural changes on HS might result in altered functionalities of the proteins with which they interact. This might contribute to altered physiological states and decline of tissue homeostasis. In myocardium, a number of GAG-binding growth factors have been directly associated with normal heart function and/or

---

[3] The abbreviations used are: ECM, extracellular matrix; DMMB, 1,9-dimethylmethylene blue; FGF, fibroblast growth factor; FGFR-1, FGF receptor type 1; GAG, glycosaminoglycan; HB-EGF, heparin-binding EGF-like growth factor; HS, heparan sulfate(s); HUVEC, human umbilical vein endothelial cell; VEGFR-2, VEGF receptor 2; VSV, vesicular stomatitis virus.

with the response of heart to injury. Among them, acidic and basic fibroblast growth factors (FGF-1 and FGF-2, respectively) and vascular endothelial growth factor (VEGF) are potent effectors of cell proliferation, mesoderm development, and vascular growth. FGF-1 is a powerful mitogen on numerous different cell types and plays roles in angiogenesis and wound healing (6, 7). FGF-2 exerts acute and direct prosurvival effects during or after an ischemic insult to heart and is now considered as a natural mediator of cardioprotection (8). VEGF, the activity of which is also regulated by HSs, accounts among the most powerful modulators of physiological and pathological angiogenesis (9). The therapeutic and cardioprotective potential of FGFs and VEGF has brought these factors to clinical trials alone, associated with cell therapies, or as their related gene therapies (9). However, even if these approaches have proven to be of some benefit in numerous animal models of myocardial ischemia, their success in clinical trials has been conditioned by multiple limitations, including poor bioavailability, side effects, and symptomatic patients (10, 11). This suggests that considerable improvements are still necessary for a real benefit, at least in the cardiovascular field.

Because GAGs are major components of the ECM in which they protect and potentiate the activities of resident and therapeutic growth factors, changes in GAG structures as consequence of tissue injury, disease, or aging could then affect the cardioprotective potential of such growth factors. Here, we investigated whether the physiological aging process can effectively induce structural changes on the endogenous myocardial GAGs and whether these changes could consequently alter the activity of growth factors known to be involved in the control of heart tissue homeostasis. GAGs were extracted from myocardium left ventricle of differently aged rats. The left ventricle was studied because of its high clinical significance in total cardiac function; its dysfunction is involved in the final pathway of myocardial infarction and other cardiac disorders. Thus, we investigated the age-related changes of the left ventricle GAG structures and capacities to bind to FGF-1, FGF-2, VEGF, and HB-EGF. The effect of the myocardial GAGs on the mitogenic activity of FGF-2 and VEGF was evaluated in cultured BaF32 and HUVEC cells, respectively, and by an angiogenic test of Matrigel plugs supplemented with myocardial GAGs and VEGF. Disaccharide analysis and immunostaining were used to approach fine structural aspects. Our results show that GAG structures are altered in the aged left ventricle and that this can significantly and differently alter the GAG capacities to potentiate growth factor functions. This study suggests the importance of myocardial GAGs qualities in age-associated heart dysfunction.

EXPERIMENTAL PROCEDURES

Animals and Tissue Dissection—Four groups of 4-, 12-, 18-, and 24-month-old male Wistar rats (Janvier) were included in the study ($n = 7$). Just before sacrifice, anesthesia was induced by intraperitoneal injection of sodium pentobarbital (50 mg/kg). The heart left ventricle and a leg extensor digitorum longus muscle were dissected after collecting blood in EDTA-containing tubes. Tissues were frozen under liquid nitrogen vapors and stored at $-80\,°C$. Experiments were conducted in conformity with the Guiding Principles for Research Involving Animals and Human Beings.

GAG Rapid Extraction and Quantification—An efficient and rapid method for GAG extraction and quantification was developed on rat left ventricle. Method details and validation are described in the supplemental materials. For control experiments, GAGs from extensor digitorum longus skeletal muscle and total blood were also extracted and quantified following similar procedures. Briefly, frozen tissues were powdered, weighed, and suspended to 25 mg/ml in the extraction buffer (50 mM Tris-HCl, pH 7.9, 10 mM NaCl, 3 mM $MgCl_2$, and 1% Triton X-100) at 4 °C. Samples were treated with proteinase K (Merck; 50 μg/ml final sample concentration) at 56 °C, overnight. After proteinase K inactivation (90 °C, 30 min), samples were treated by DNase (Qiagen; 30 units/ml final sample concentration) at 37 °C, overnight. Samples were then centrifuged (13,000 $\times$ g, 20 min), and supernatants were recovered. Pellets were shown to be free of GAGs and discarded. Then, 10 –100 μl of the filtered proteinase K/DNase-digested samples (adapted for a maximum of 5 μg of GAGs expected in sample) were adjusted to 100 μl of final volume with water. To each sample, 1 ml of the GAG-complexing 1,9-dimethylmethylene blue (DMMB) solution (see supplemental materials) was added, and samples were vigorously agitated. Then, samples were centrifuged (13,000 $\times$ g, 10 min) to sediment the solid GAG-DMMB complex, and supernatants were discarded. The GAG-DMMB pellet was then dissolved in 250 μl of the decomplexing solution (see supplemental materials) by vigorous shaking, and absorbance of the resulting blue solution was measured at 656 nm. A calibration curve, constructed with known amounts of standard chondroitin sulfate A ranging from 0 to 50 μg/ml (0 –5 μg/assayed sample) was included in every assay. Quality controls (see supplemental materials) were also included in every assay. Results were expressed in μg of GAG/mg of dried tissue. Extraction of GAGs was complementarily performed from the proteinase K/DNase-treated sample as detailed below.

GAG Isolation—This step is recommended when the extracted GAGs are to be used to test their functionality in biological assays or as substrates for enzymatic digestion. Briefly, proteinase K/DNase-digested samples were diluted to 2 M NaCl final sample concentration and vigorously agitated for 10 min. Proteins were precipitated, and supernatants were cleared by chloroform washing followed by rapid dialysis of the aqueous phase (Slide-A-Lyzer Mini Dialysis Units 3,500 molecular weight cut-off; Pierce) against the extraction buffer and then pure water. After freeze-drying, material was dissolved in water or in a glycanases digestion buffer (10 mM sodium acetate, 2 mM $CaCl_2$, pH 7), as required. GAGs were then quantified by following the DMMB protocol. A GAG reproducible loss of 10 –15% during the isolation procedure was observed. Identities of the extracted GAGs were confirmed by specific digestion with chondroitinase ABC, heparinases I/II/III, or by nitrous acid treatment as previously described (12) (for method details and validation see supplemental materials).

Heparin versus GAG Competition Assay toward Growth Factors—ELISA plates were coated with a 2 μg/ml BSA-heparin conjugate solution prepared as described previously (13). After washing (0.05% PBS and Tween 20), wells were saturated

with 3% BSA in PBS. Then, the studied growth factor (R&D Systems) was added to the plate at various concentrations (0, 5, 10, 25, 50, 100, 200, and 500 ng/ml) to determine the protein concentration giving 50% binding to immobilized heparin. Working growth factor concentrations were then fixed at 50 ng/ml for FGF-1, FGF-2, and HB-EGF and 180 ng/ml for VEGF. These concentrations were used to determine the capacity of competing soluble extracted GAGs (0, 0.1, 0.5, 1, 5, 10, 50, 100, 500, and 1000 ng/ml in PBS) to inhibit the growth factor binding to the immobilized heparin. For the test, growth factors and extracted GAGs were simultaneously added to the wells. After a 1-h incubation at room temperature, wells were washed, and the growth factor remaining bond to heparin was detected by incubation with the corresponding primary antibody (R&D Systems) followed by a peroxidase-labeled secondary antibody (Jackson Laboratories). Peroxidase activity measurement was performed with the 3,3′,5,5′-tetramethylbenzidine substrate of the Peroxidase Activity Detection kit (Pierce) following fabricant indications. Efficient concentration of GAGs from 4-month-old rat left ventricle required to bind the assayed growth factor was considered as reference binding (100%).

FGF-2- and GAG-dependent Mitogenic Activity Assay— BaF32 cells were maintained as described previously (14). For the assay, cells were seeded into 96-well plates at a density of 50,000 cells/well in RPMI 1640 medium supplemented with 10% horse serum and, otherwise specified, with 5 ng/ml FGF-2 and the extracted GAGs at various concentrations (0.1, 1, and 10 μg/ml). Heparin (2 μg/ml; Sigma) was used as a positive control (14). The FGF-2 working concentration was selected from the linear region of a FGF-2 dose-response curve (0, 2.5, 5, 25, and 50 ng/ml) in the presence of 2 μg/ml heparin. After a 48-h incubation at 37 °C, cells were labeled with [^{3}H]thymidine for 5 h, and the metabolic labeling was terminated by harvesting the cells on a filtermate 196-cell harvester Dynatech (Bioblock). Cells were then treated in Optiphase Hisafe 3 solution (PerkinElmer Life Sciences), and incorporated radioactivity was determined by liquid scintillation counting on a top counter 1450 Microbeta (Wallac). The mitogenic effect obtained with control (2 μg/ml heparin and 5 ng/ml FGF-2) was used as reference effect (100%) for comparative purposes.

*VEGF-dependent Mitogenic Activity Assay—*HUVECs were routinely maintained at 37 °C, 5% CO_2 in EBM-2 BulleKit medium (Lonza) containing 2% FBS and EGM-2. For the assay, HUVECs were seeded into 24-well plates at a density of 30,000 cells/well in growth medium supplemented with SingleQuots according to the manufacturer's instructions (Lonza). Cells were incubated overnight at 37 °C, and then the medium was replaced into starvation EMB-2 medium containing 0.5% FBS. Cells were again incubated for 24 h at 37 °C in 5% CO_2. GAGs were then added to wells at final concentrations of 0.3, 3, or 30 ng/ml (15) in the presence, or not, of VEGF$_{165}$ (3 ng/ml), and cells were incubated for an additional 24 h. Phase contrast images of cultures were taken by an Axiovert 10 microscope (Zeiss). Cells were then fixed with absolute ethanol, and the amount of cells in dishes was evaluated by crystal violet staining (16). Heparin (3 ng/ml) was used as a positive control, and its effect was considered as 100% effect (15).

*Matrigel Plug Assay and VEGFR-2-expressing Cell Staining—*Liquid Matrigel (0.3 ml) at 4 °C was subcutaneously injected into Swiss mice (Janvier) ($n = 3$) alone or supplemented with VEGF$_{165}$ at 50 ng/ml final concentration and in the presence or absence of extracted GAGs (3 ng/ml), one plug by mice, as described previously (15). Mice were sacrificed after 8 days, skin was pulled back, and plugs were excised and frozen in liquid nitrogen. Cryosections of 8-μm thickness were prepared and fixed with acetone. For VEGFR-2 immunostaining, slides were rehydrated in 1% BSA and 2% goat serum in PBS followed by incubation with an anti-VEGFR-2 polyclonal antibody. VEGFR-2 was revealed by avidin-biotin alkaline phosphatase staining (Vector Laboratories). Briefly, slides were incubated with biotinylated goat anti-rabbit IgG for 1 h at room temperature, washed, and incubated again with an avidin-biotinylated alkaline phosphatase complex following revelation by alkaline phosphatase red substrate as indicated by the manufacturer. Nuclear staining was done by a 5-min incubation with 1 μg/ml DAPI followed by PBS washing. Images were obtained using a CCD monochrome camera (CFW-1310M; Scion Corporation) fitted to a BH-2 epifluorescence optical microscope (Olympus). Image processing and analysis were done using the ImageJ software (National Institutes of Health) (17). Nuclei labeling was quantified as described previously using ImageJ (18).

*Myocardial GAG Immunostaining—*Tissue cryosections (8 μm) were fixed with 4% paraformaldehyde, washed, incubated for 2 min with 50 mM NH$_4$Cl in PBS, and washed again. Sections were saturated with 3% BSA/PBS for 1 h. GAGs were then stained with different phage display antibodies (1:5) (see Fig. 6 for antibodies identities and references). Immunolabeling was carried out overnight at 4 °C. A mouse anti-VSV tag IgG antibody P5D4 (1:200) followed by incubation with a secondary antibody conjugated to the Alexa Fluor 488 fluoroprobe (Molecular Probes; 1:200 dilution) was used to reveal GAG staining. Tissue sections were then incubated with 1 μg/ml DAPI for 5 min and rinsed. Images were obtained as described above.

*Heparan Sulfate Isolation—*Chondroitinase ABC was used to selectively digest chondroitin sulfates from isolated GAG samples. Briefly, samples in the glycanase digestion buffer were incubated with 10 milliunits of chondroitinase ABC (1 h, 30 min at 37 °C). Digested chondroitin sulfate saccharides were removed from samples by rapid dialysis against water. Complete digestion of chondroitin sulfate and stability of the HS fraction under the experimental conditions were controlled by treating, at the same time, commercially available chondroitin sulfates and HS standards. HS samples were lyophilized and stored at −20 °C until use.

*Heparan Sulfate Disaccharide Analysis—*HS lyophilized samples were suspended in the digestion buffer and simultaneously treated with heparinase I, II, and III mixture (0.25 milliunit each, 24 h, 37 °C). After filtration, samples were injected to an HPLC system and analyzed as described previously (19) with some modifications. Briefly, a 20-μl sample was automatically loaded onto a Propac PA-1 strong anion exchange column (4.6 × 250 mm; Dionex) eluted by a solvent gradient consisting of eluent A (NaCl 100 mM) and eluent B (NaCl 1 M) each at 0.25

ml/min flow rate. The gradient was 0–5 min (0% B), 5–20 min (0–50% B), 20–25 min (50–100% B), 25–30 min (100% B), 30–35 min (100–0% B), and 35–40 min 0% B. The column effluent was mixed in line with 2% of 2-cyanoacetamide solution and a 250 mM NaOH solution, both individually supplied at 0.25 ml/min each. The mixture passed through a reaction coil (10-m length, 0.5-mm internal diameter) set in an oven at 120 °C, followed by a cooling coil (3-m length, 0.25-mm internal diameter). The effluent was monitored at 346 nm of excitation and 410 nm of emission with a fluorescence detector (JASCO; FP-1520). Unsaturated disaccharides ΔUA-GlcNAc, ΔUA-GlcNS, ΔUA-GlcNAc6S, ΔUA2S-GlcNAc, ΔUA-GlcNS6S, ΔUA2S-GlcNS, ΔUA2S-Glc-NAc6S, and ΔUA2S-GlcNS6S (Iduron Ltd.) were used as standards for peak identification. Areas under the peaks were measured, and the percentage of each disaccharide in sample was calculated. The disaccharide composition was expressed in molar %. Complete HS digestion under the experimental conditions was controlled by treating, in parallel with samples, commercially available HS and heparin standards. Five samples from rat left ventricle were analyzed by group ($n = 5$).

Statistical Analysis—Values are expressed as mean ± S.D. ($n = 7$ or $n = 5$ as indicated). The statistical significance of differences between various groups was determined by one-way analysis of variance, and group-to-group comparisons were made by a two-tailed unpaired Student's t test (GraphPad Prism 5). Samples from each animal were analyzed three times as triplicates. A p value < 0.05 was considered to be statistically significant. Note that *, ≤0.05; **, ≤0.01; and *** ≤0.001.

RESULTS

Extraction and Quantification of GAGs from Rat Heart Left Ventricle—As a part of this work, we developed an efficient method for total sulfated GAG extraction from heart tissue and for their accurate quantification. Method details and validation procedures for linearity, precision, and accuracy in rat left ventricle samples spiked with chondroitin sulfate A are described in supplemental materials. Intra-day and inter-day linearities were, respectively, $r^2 = 0.9965$ and $r^2 = 0.9961$ for a range of 0–6.5 μg of GAGs in the analyzed samples. Precision, or relative standard deviation (%CV), was 3.6% for intra-day and 5.4% for inter-day analyses. Accuracy, or the exactness of the method corresponding to the relative percentage of recovery from the theoretical analyte concentration on spiked samples ($n = 3$), was 95.8–99.3%. Limits of detection and quantification were 100 and 250 ng, respectively. The validated method was thus suitable for analysis of heart tissue.

GAG Levels Increase with Age in Rat Myocardium—Application of the GAG extraction/quantification method to the analysis of myocardium showed that the 24-month left ventricle GAGs increased of 37.1% (from 0.56 to 0.76 μg/mg tissue) compared with those in 4-month-old tissue (Fig. 1A). This increase in sulfated GAGs appeared specific to myocardium because GAG levels were kept constant between 4 and 24 months in blood and were only slightly increased in skeletal muscle (Fig. 1B). These results indicate that endogenous total sulfated GAG levels increase progressively in myocardium during the physi-
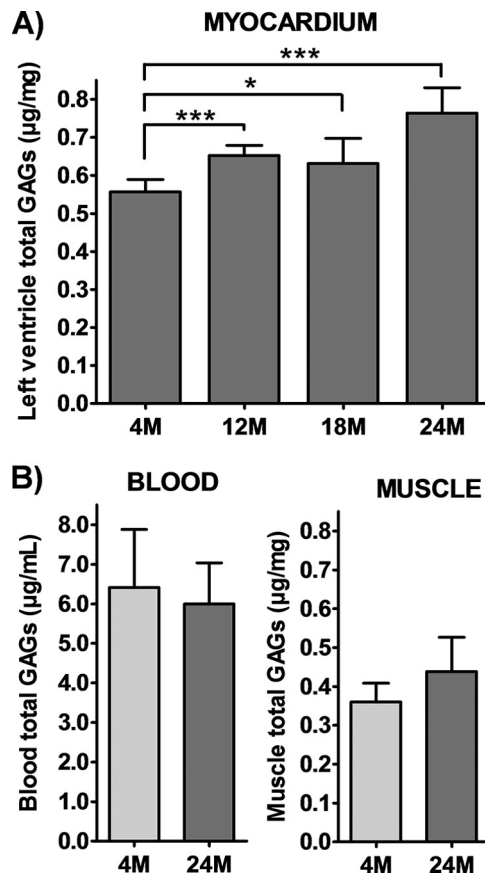

FIGURE 1. **Total sulfated GAGs content in aging myocardium.** Total sulfated GAGs were extracted and quantified according to the validated extraction/quantification method detailed in supplemental materials. GAG levels were normalized in μg of total GAGs by mg of dried tissue. *A*, total sulfated GAGs levels in 4- (*4M*), 12- (*12M*), 18- (*18M*), and 24-month-old rat (*24M*) myocardium left ventricle. *B*, total blood and skeletal (extensor digitorum longus) muscle total GAGs from the same 4- and 24-month-old rats. The values are the means of seven rats of same age in each group. The *error bars* represents mean ± S.D. ($n = 7$). The data are representative of three separate experiments. *, $p ≤ 0.05$; ***, $p ≤ 0.001$.

ological aging process and that the age-related modifications of GAG levels differ among tissues.

GAGs from Aged Myocardium Exhibit Altered Capacities to Bind Different Growth Factors—To compare the ability of 4- and 24-month myocardial GAGs to bind different growth factors including FGF-1, FGF-2, HB-EGF, and VEGF$_{165}$, we used a competition ELISA. This assay was based on the capacity of GAGs to inhibit the binding of the assayed growth factor to heparin. Table 1 shows the myocardial GAG concentrations required to inhibit 50% (EC$_{50}$) of the growth factors binding to immobilized heparin. These results show that, with aging, the GAG affinities for FGF-1 and FGF-2 significantly decrease whereas they increase for VEGF$_{165}$ and remain unchanged for HB-EGF. These changes in GAG affinity for growth factors might reflect GAG structural and functional changes.

Aging Decreases Myocardial GAG Capacities to Potentiate FGF-2 Mitogenicity—To investigate whether aging changes the capacity of GAGs to potentiate growth factor activities we first used a mitogenic activity assay on BaF32 cells, a lymphoblastoid cell line transfected with the FGF receptor type 1 (FGFR-1). These cells are devoid of cell surface HS and respond to FGF-2

TABLE 1

Relative 4- *versus* 24-month-old rat myocardial GAGs capacities to bind growth factors

	Myocardial GAG IC_{50}[a]	
Growth factor	4 Months	24 Months
	ng/ml	*ng/ml*
FGF-1	6.6 ± 1.0	10.4 ± 1.0*
FGF-2	38.0 ± 3.2	56.6 ± 3.2*
FGF-2 to LV HS[b]	30.0 ± 0.8	46.2 ± 2.2**
HB-EGF[c]	18.0 ± 2.2	19.2 ± 1.6
$VEGF_{165}$	11.0 ± 0.6	3.4 ± 1.6**

[a] IC_{50}, GAG concentration needed to effectively inhibit 50% of the growth factor binding to immobilized heparin. *, $p \leq 0.05$; **, $p \leq 0.01$.

[b] FGF-2 to LV HS, left ventricle (LV) and heparan sulfate (HS) were used instead of total GAGs to inhibit the FGF-2 binding to heparin.

[c] HB-EGF, heparin-binding EGF-like growth factor.

only in the presence of exogenous GAGs or heparin (14). Fig. 2*A* shows that myocardial GAGs from the 24-month rats have reduced capacities to stimulate FGF-2-dependent BaF32 proliferation compared with the 4-month-GAGs, as demonstrated by a dose-dependent reduced [³H]thymidine incorporation. Fig. 2*B* shows the age-dependent binding of the myocardial GAGs to FGF-2. These results indicate that aging causes a decrease in the myocardium GAG capacities to potentiate FGF-2 activity.

Aging Induces Increased Myocardial GAG Capacities to Potentiate $VEGF_{165}$ Activity—In contrast with the age-related reduced binding of myocardial GAGs to FGF-2, our results showed that they can bind more efficiently to $VEGF_{165}$ (Table 1). We thus compared the capacities of the 4- and 24-month GAGs to induce $VEGF_{165}$-dependent mitogenic effect on HUVECs. In accordance with the binding experiments, $VEGF_{165}$ was more efficient at triggering HUVEC proliferation in the presence of the 24-month left ventricle GAGs than in the presence of the 4-month GAGs (Fig. 3). This $VEGF_{165}$ potentiating effect was confirmed in a Matrigel angiogenic assay in mice in which VEGFR-2-expressing cells were immunologically labeled in plugs supplemented with the 4- or 24-month myocardial GAGs and with $VEGF_{165}$. Fig. 4 shows a significant increase of VEGFR-2-expressing cells in the 24-month GAG-treated plugs. Thus, as age advances, the angiogenic potential of myocardial GAGs increases.

Heparan Sulfates Are Responsible for Total GAG Level Increase in Aged Myocardium—To investigate the differential contribution of myocardial GAG species in some of the observed effects, we performed selective chondroitinase ABC or/and nitrous acid digestions of total GAG extracts. Our results show that HS species increase with aging, from 406 ng/mg tissue at 4 months to 534 ng/mg at 24 months (32%, $p < 0.001$), whereas the levels of chondroitin sulfates remained unchanged (Fig. 5*A*). Samples digested with chondroitinase ABC followed by nitrous acid treatment completely erased all GAG signals, indicating that HS and chondroitin sulfates are the major GAG species in this tissue (Fig. 5*A*). Thus, the increase of GAGs observed in the aged myocardium can be associated with an age-related increase of HS in this tissue.

Heparan Sulfates from Aged Myocardium Show FGF-2 Binding Alterations—We then investigated whether the isolated HS fraction could reflect the age-dependent decrease on FGF-2
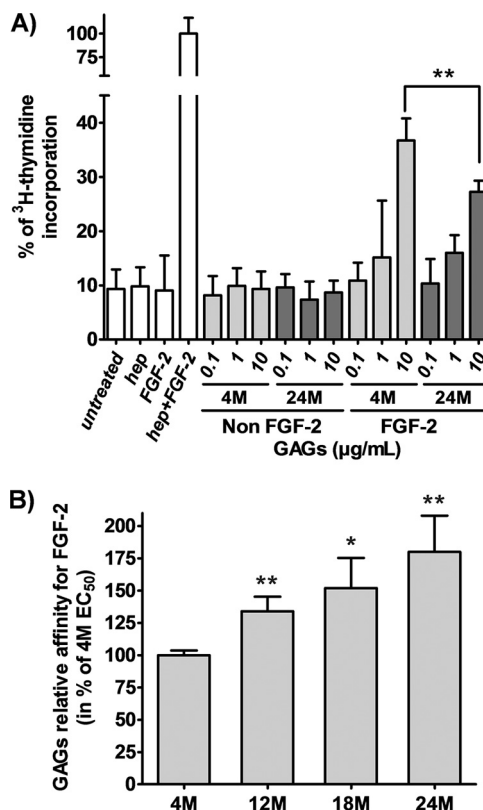
FIGURE 2. **Aging decreases myocardial GAG capacities to potentiate FGF-2 mitogenic activity and binding.** *A*, relative capacity of 4-month-old (*4M*) *versus* 24-month-old (*24M*) myocardial GAGs to induce FGF-2 mitogenic activity assessed by [³H]thymidine incorporation in FGFR-1-transfected BaF32 cells (14). For comparison experiments, myocardial GAGs (0.1, 1, and 10 µg/ml) were tested in the presence and in the absence of FGF-2 (5 ng/ml). This FGF-2 concentration was selected from the linear region of a FGF-2 dose-response curve (0, 2.5, 5, 25, and 50 ng/ml) obtained in the presence of 2 µg/ml commercial heparin (*hep*) (data not shown). The effect of heparin (2 µg/ml) in the presence of FGF-2 (5 ng/ml) was considered as a positive control (100%) (14). *B*, age-related changes on the myocardial GAG relative affinities for FGF-2. EC_{50} corresponds to the GAGs concentration required to inhibit 50% of FGF-2 binding to immobilized heparin as assessed by a competition ELISA. For the assay, the growth factor (50 ng/ml) and the myocardial GAGs (0, 0.1, 0.5, 1, 5, 10, 50, 100, 500, and 1000 ng/ml) were incubated in heparin-coated ELISA plates. After washing, the growth factor remaining in the plate was immunologically assessed to determine the level of FGF-2 bound to GAGs. The used FGF-2 concentration was selected from the linear region of a dose-response (0, 5, 10, 25, 50, 100, 200, and 500 ng/ml) curve of the FGF-2 binding to immobilized heparin. For comparison experiments, 4-month-old GAG EC_{50} was considered as reference response (100%). 0 response was that obtained in the absence of competing GAGs. Data are the mean ± S.D. (*error bars*) for seven animals (myocardial GAGs) in each group ($n = 7$). Experiments were repeated three times with similar results. *, $p \leq 0.05$; **, $p \leq 0.01$.

binding observed with total GAGs. Fig. 5*B* shows that 24-month myocardial HS have a decreased affinity for FGF-2 as reflected by the increased concentration needed to effectively inhibit 50% of the growth factor binding to immobilized heparin (EC_{50}). These results indicate that HS in the aged myocardium have altered capacities to bind to the growth factor.

Immunostaining of Myocardial Heparan Sulfates—To confirm the age-dependent increase of HS levels in myocardium, we performed immunohistological staining of tissue slides with several phage display antibodies. From the panel of used antibodies (Fig. 6), AO4B08, NS4F5, and RB4Ea12, raised against HS, stained the cardiac muscle with clear higher intensity in the aged tissue. The antibody AO4B08 is known to stain adult tis-
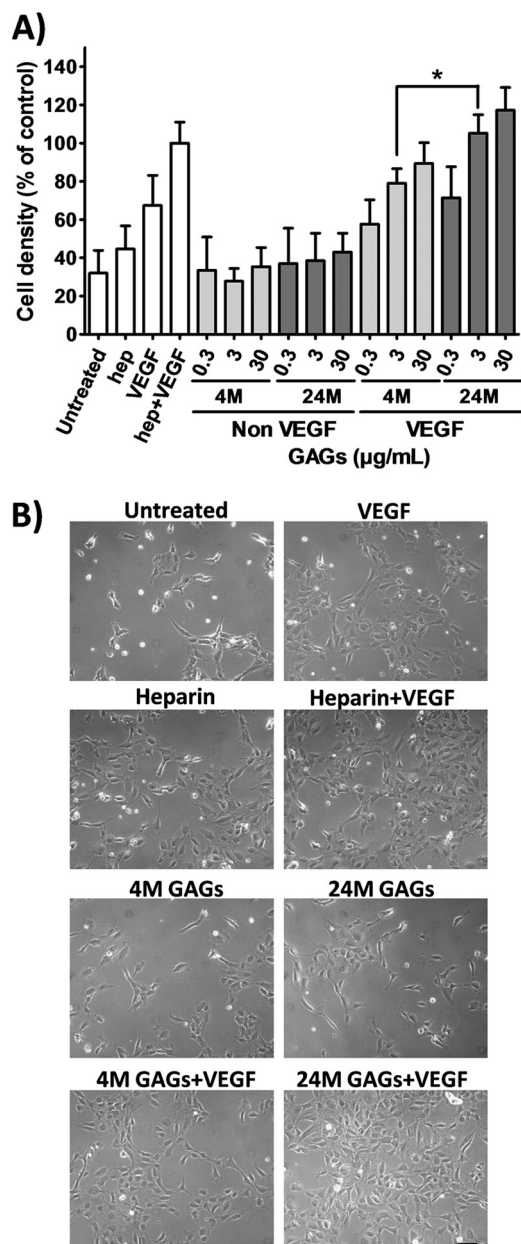
FIGURE 3. **Aging increases myocardial GAG capacities to potentiate VEGF_{165} mitogenicity on HUVECs.** The relative capacity of 24-month-old (*24M*) versus 4-month-old (*4M*) myocardial GAGs to promote VEGF signaling was examined in a proliferation assay using HUVECs. Cells were cultured as described under "Experimental Procedures." *A*, 4- and 24-month-old rat myocardial GAG (0.3, 3, and 30 ng/ml) capacities to induce HUVEC proliferation, as assessed by crystal violet staining, in the absence or in the presence of VEGF_{165}. As positive control (100%), HUVECs were cultured in the present of heparin (3 ng/ml) and VEGF_{165} (15). Data shown are from a single experiment (mean ± S.D. (*error bars*), n = 7) representative of three repeated experiments. *, $p \leq 0.05$. *B*, representative experiment of HUVEC growth in control conditions and in the presence of 4- and 24-month-old rat myocardial GAGs (3 ng/ml) and VEGF_{165} (3 ng/ml) after 24 h of cell growth. *Scale bar*, 50 μm.

sues ubiquitously and characteristically to recognize NS domains in HS with 6-O-sulfation-dependent binding (20, 21). Antibody NS4F5, which also recognizes NS domains, has shown restricted staining in adult tissues and is known to recognize regions with endothelial cell activation (21, 22), its binding is favored by 6-O-sulfation. Antibody RB4Ea12 characteristically recognizes NA/NS domains in which 6-O-sulfation also

favors binding (21, 23). Anti-HS antibodies that failed to stain myocardial muscle included LKiv69, EV3C3, and HS4C3. Antibody LKiv69 recognizes *N*- and 2-*O*-sulfated sequences, and 6-*O*-sulfation is known to reduce binding (21, 24). EV3C3 also recognizes *N*- and 2-*O*-sulfated sequences, and 6-*O*-sulfation is also known to reduce binding (25). Antibody HS4C3, raised against heparin, characteristically recognizes highly sulfated NA/NS domains, but 3-*O*-sulfation is required for binding (21, 26). Among antibodies raised against chondroitin sulfates, positive staining was only observed with the anti-dermatan sulfate LKN1, which recognizes GlcA2S-GalNAc4S (27). However, no differential staining with this antibody was observed between the young and old tissues. Among the antibodies raised against chondroitin sulfates that failed to stain myocardium are IO3H10, specific for chondroitin 6-*O*-sulfate (28); GD3A12, specific for dermatan sulfate with characteristic IdoA-GalNAc4S recognition and in which IdoA is required for binding and eventually 6-*O*-sulfation reduces binding (29); and GD3G7, which recognizes chondroitin sulfate E containing IdoA-GalNAc4S6S (30).

Overall, a higher labeling in the 24-month myocardium compared with the 4-month one was observed with the anti-HS antibodies that efficiently stained this tissue. In most cases, staining was probably linked to a high 6-*O*-sulfation content. Antibodies that failed to stain were mainly those requiring low 6-*O*-sulfation or the presence of 3-*O*-sulfated species.

A fine analysis of merged phase contrast and AO4B08 fluorescence images (Fig. 7A) showed that HS labeling on the aged tissue was more diffuse and disorganized among the cardiac muscle fibers compared with the young tissue. Interestingly, this disorganization was accompanied by an increase of HS aggregate-like spots (Figs. 6 and 7A). Fig. 7B shows a further normalization of the HS fluorescent signal (AO4B08) by the amount of DAPI-stained nuclei. This shows that the increased fluorescent signal is not due to an increased number of cells, observed in some areas of the aged tissue, but more likely to an increased production or accumulation of the polysaccharide in the aged tissue. Together, these observations suggest that aging induces changes in the HS composition, organization, and deposition in myocardium left ventricle.

Disaccharide Analysis of Heparan Sulfate from Aged Rat Left Ventricle Shows Altered Sulfation—To investigate whether aging induces changes on myocardial HS structures, we performed disaccharide analysis of the HSs from 4- and 24-month left ventricles. Fig. 8 shows that the levels of specific HS disaccharides are modified in myocardium from the 24-month animals compared with those from the young animals. Among the monosulfated disaccharides a significant decrease of the *N*-sulfated ΔUA-GlcNS disaccharide was observed (↓ NS). Although observed in a very small relative content, the level of 2-*O*-sulfated ΔUA2S-GlcNAc disaccharide appeared also decreased (↓ 2S). This contrasted with the important increase of the 6-*O*-sulfated ΔUA-GlcNAc6S disaccharide (↑ ↑ 6S). Consistently, the aged tissue showed significantly increased ΔUA-GlcNS6S (↑ ↑ NS,6S) and slightly decreased ΔUA2S-GlcNS (↓ 2S,NS) disulfated disaccharides levels. Moreover, the trisulfated disaccharide ΔUA2S-GlcNS6S, characteristic of NS domains, although present in low levels, was found slightly increased in
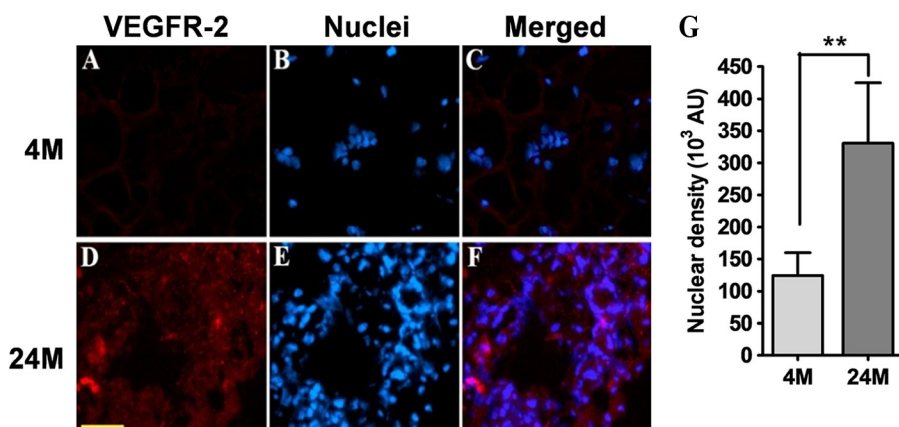
FIGURE 4. **Aging enhances myocardial GAGs angiogenic potential.** VEGFR-2-expressing cells in Matrigel plugs implanted in mice were analyzed by immunological staining of 8-μm Matrigel cryosections (see "Experimental Procedures"). Prior to implantation, Matrigel was treated with $VEGF_{165}$ (50 ng/ml final concentration) together with 4- (*4M*) or 24-month-old (*24M*) rat myocardial GAGs (3 ng/ml final concentration) (15). *A–C*, respectively, VEGFR-2, DAPI, and merged images from 4-month-old GAG- and $VEGF_{165}$-supplemented plugs. *D–F*, equivalent images obtained from 24-month-old GAG- and $VEGF_{165}$-supplemented plugs. VEGFR-2 was revealed by avidin-biotin alkaline-phosphatase staining (*red*). Nuclei staining are in *blue* (DAPI). Shown microphotographs are from a single representative set of animals. *Scale bar*, 50 μm. *G*, nuclear density expressed in arbitrary units (*AU*) as determined by image analysis using the ImageJ software (17). Histograms represent the effect of three rat myocardial GAGs extracts tested by age group (mean $\pm$ S.D. (*error bars*), $n = 3$; **, $p \leq 0.01$) in which each myocardial GAG extract was tested in three independent mice with one plug by recipient mice.
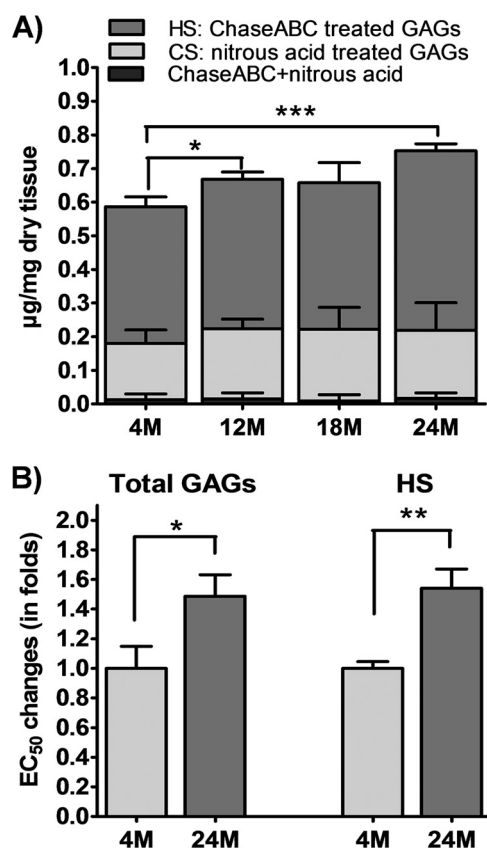

FIGURE 5. **Myocardial HS levels and FGF-2 binding abilities change with aging.** *A*, age-related changes of HS and chondroitin sulfate (*CS*) levels in left ventricle. HS were quantified after chondroitinase ABC digestion (*dark gray bars*) and CS after nitrous acid treatment (*light gray bars*) of total GAGs extracts as described under "Experimental Procedures." GAG levels after chondroitinase ABC and nitrous acid consecutive digestions are also represented (*black bars*). *B*, 4- (*4M*) and 24-month-old (*24M*) myocardial HS capacities to inhibit the FGF-2 (50 ng/ml) binding to immobilized heparin as assessed by competition ELISA. Data are the mean $\pm$ S.D. (*error bars*) for five animals in each group. Data shown are from a single experiment and representative of two separated experiments. *, $p \leq 0.05$; **, $p \leq 0.01$; ***, $p \leq 0.001$.

elder's tissue ($\uparrow$ 2S,*N*S,6S) (Fig. 8). ΔUA2S-GlcNAc6S was not detected. Overall, these results show that the age-dependent increase of HS in left ventricle is accompanied by structural changes involving enhanced 6-*O*-sulfation, reduced *N*-sulfation, and likely reduced 2-*O*-sulfation. This translates into an age-dependent alteration of the enzymatic machinery regulating HS biosynthesis.

DISCUSSION

It is now well accepted that ECM plays a major role among factors ruling tissue integrity and homeostasis, offering to cells not only an optimal mechanical environment to survive but also the necessary signals to growth, to differentiate, to move, and to respond to stress. Thus, the quality of the ECM can influence the function of a complete set of chemical signals and tissue remodeling effectors including growth factors, inflammatory cytokines, matrix metalloproteinases, and enzymes (1). Although GAGs account among the main ECM effectors known to regulate the activity of several of these proteins, in heart, most efforts have been essentially focused to the study of matrix protein components (31) possibly because of the lateness of methods allowing the study of glycans. As a part of this work, we have developed and validated an efficient method for total sulfated GAG extraction from heart tissue and for their accurate quantification. This method allowed us to show that, with aging, total sulfated GAGs are increased in rat left ventricle and that this increase concerns essentially HS species.

That HS increase in the aged tissue was confirmed by immunohistological staining with a battery of phage display anti-GAGs antibodies which differential labeling gave additional information on the HS domains expressed in myocardium. These domains included NS domains recognized by antibodies AO4B08 and NS4F5, and NA/NS domains, recognized by the RB4Ea12 antibody. Typically, NS domains are composed of contiguous *N*-sulfated disaccharide units that may carry both 6-*O*- and 2-*O*-sulfate groups, whereas NA/NS domains are characteristically composed of alternating *N*-acetylated and
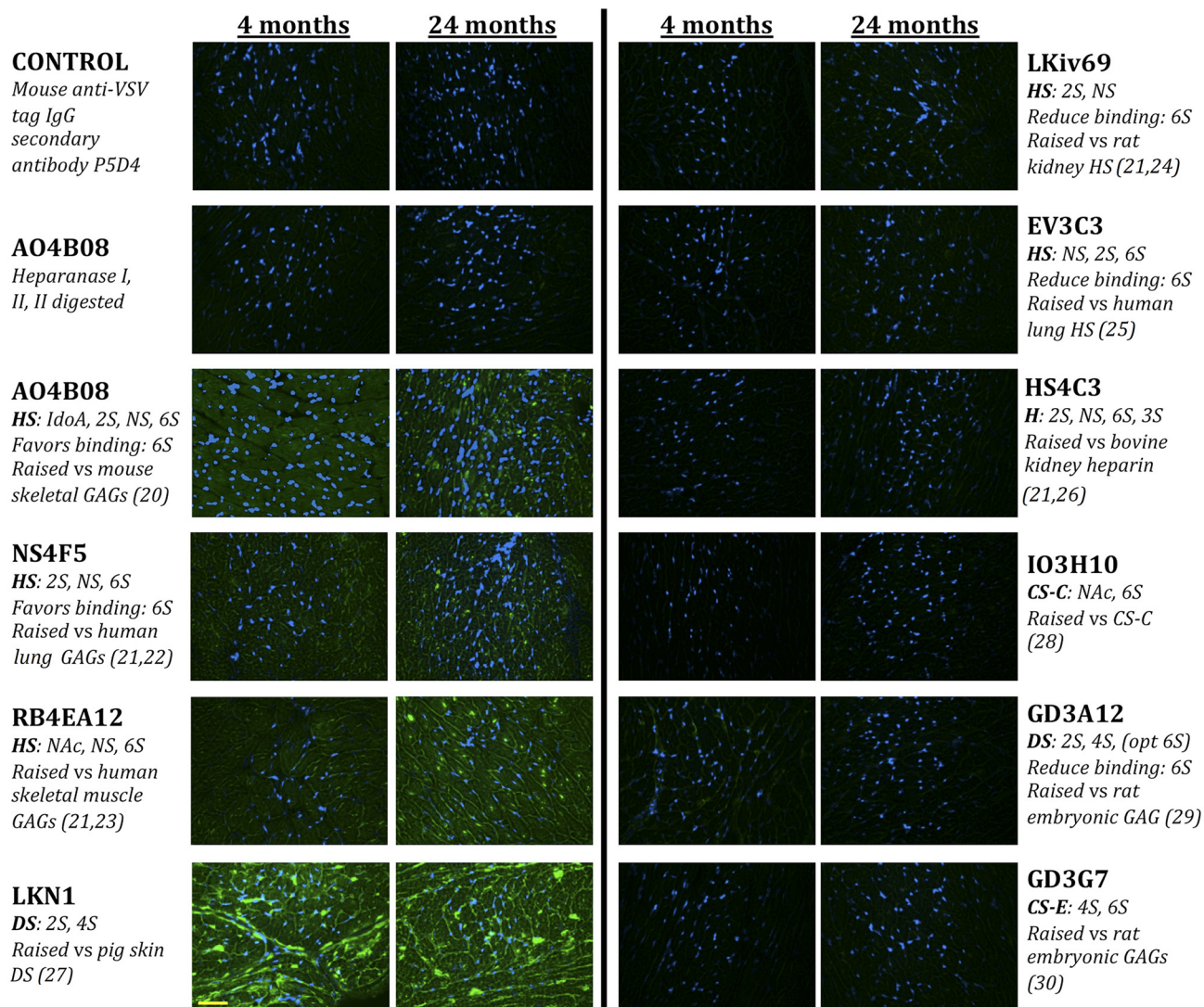
FIGURE 6. Aging increases HS labeling with phage display antibodies in left ventricle. Fixed cryosections from 4- and 24-month-old rat left ventricle were incubated with the indicated phage display antibody. Bound antibodies were detected by incubation with mouse anti-VSV tag IgG antibody P5D4, followed by Alexa Fluor 488-conjugated goat anti-mouse IgG (*green*) and by DAPI for staining of nuclei (*blue*). Some reference describing the antibodies specificities are given in *parentheses*. *CS*, chondroitin sulfate; *IdoA*, iduronic acid; *hep*, heparin; *2S*, 2-O-sulfation; *NS*, N-sulfation; *6S*, 6-O-sulfation; *3S*, 3-O-sulfation. Omission of the anti-HS antibody or treatment of cryosections with heparinases I/II/III mixture (12) prior to incubation with antibody AO4B08, was used as staining controls. Specificity of other used antibodies is detailed in the given references. *Scale bar*, 50 μm.

N-sulfated units containing 6-O-sulfate groups, but lacking of 2-O-sulfate residues. The notable increased labeling upon aging with AO4B08, an antibody known to recognize sequences containing higher 6-O- than 2-O- sulfation (20, 21), suggested the presence of increased levels of 6-O-sulfated NS domains in elderly tissue. The increased 6-O-sulfation in aged heart was here confirmed by disaccharide analysis of HS. Moreover, immunostaining specificity analysis of the used antibodies set (see Fig. 6) indicates that the HS labeling was efficient with antibodies requiring high 6-O-sulfation for recognition and that staining failed with antibodies which binding is reduced by 6-O-sulfation and with those for which binding requires additional 3-O-sulfation. Together, these data reinforce the importance of 6-O-sulfotransferases and HS 6-O-endosulfatases (32, 33) in the regulation of cardiac angiogenesis. Thus, a number of reports have indicated that HS bearing high 6-O-sulfation stimulates VEGF$_{165}$-promoted

angiogenesis (34). Here, the enhanced angiogenic character of HS from the aged myocardium was suggested by the higher capacity of the corresponding GAGs to bind to VEGF$_{165}$ and to stimulate endothelial cell proliferation. Accordingly, our results showed an increased labeling with the NS4F5 antibody, which characteristically recognizes angiogenic NS domains (21, 22).

In addition to VEGF$_{165}$ altered affinity, this study shows that aging significantly reduces the capacity of the myocardial GAGs to bind FGF-1 and FGF-2. This might result from changes in the sulfation patterns of the HS polymer chain. Accordingly, previous reports outline the importance of specific sulfations on the binding of HS to FGF-1, FGF-2 and to their receptors (34–36). Because these growth factors are regulators of cell proliferation and myocyte differentiation, their decreased activities mediated by HS structural alterations in aged tissue could be involved in heart function impairment.
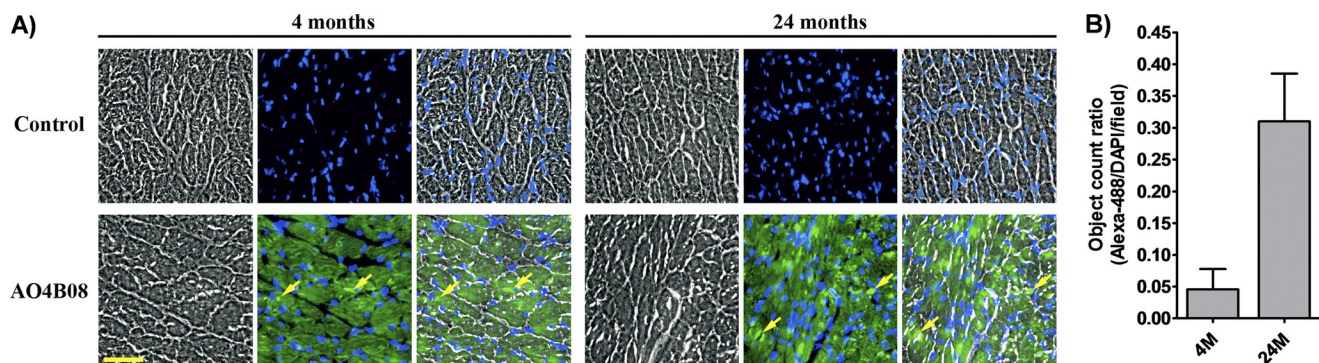
FIGURE 7. **Age-related changes in the HS spatial distribution and aggregate-like deposition.** Fixed myocardium cryosections from 4- and 24-month-old rats were incubated with the antibody AO4B08. Antibody labeling was detected by incubation with mouse anti-VSV tag IgG antibody P5D4 followed by Alexa Fluor 488-conjugated goat anti-mouse IgG (*green*) and by DAPI for nuclei staining (*blue*). To improve localization of the green signal, images were normalized between the mean value of the antibody control and the maximum encountered value in each image. *A upper*, phase contrast (*gray*) and nuclei staining (*blue*) images of 4- and 24-month-old rat tissue in which AO4B08 antibody was omitted (control). *Lower*, phase contrast (*gray*), AO4B08 staining (*green*), and nuclei staining (*blue*) of 4- and 24-month-old rat tissue. HS aggregate-like spots are indicated (*yellow arrows*). Fluorescent and phase contrast apparent co-localization were performed using a previous work adapted to ImageJ. All of the images are at the same magnification. *Scale bar*, 50 μm. *B*, average object count ratio corresponding to the number of *green* objects (AO4B08) divided by the number of *blue* objects (DAPI) counted on the same fields. The area of the counted objects was determined by image analysis using the ImageJ program (17). Data shown are from a single experiment (mean ± S.D. (*error bars*), $n = 3$). **, $p \leq 0.01$.
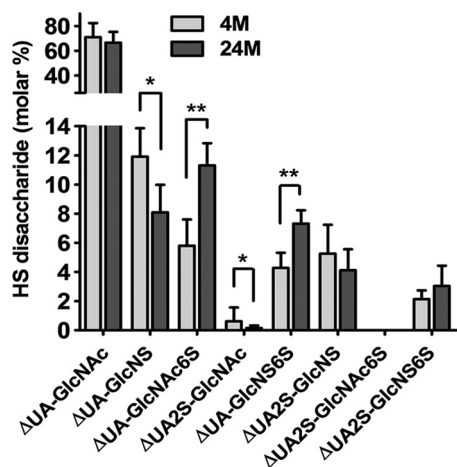

FIGURE 8. **Myocardial HS composition changes with aging.** HS isolated from 4- (*4M*) and 24-month-old (*24M*) rat left ventricles were digested with a mixture of heparin lyases (heparinase I/II/III mixture), and the resultant disaccharides were subjected to strong anion exchange chromatography in a Propac column eluted by a NaCl gradient with post-column fluorescence labeling as described under "Experimental Procedures." Unsaturated disaccharides ΔUA-GlcNAc, ΔUA-GlcNS, ΔUA-GlcNAc6S, ΔUA2S-GlcNAc, ΔUA-GlcNS6S, ΔUA2S-GlcNS, ΔUA2S-GlcNAc6S, and ΔUA2S-GlcNS6S were used as standards for peak identification. Peak areas were measured and disaccharide analysis of age-dependent HS in 4- and 24-month-old rat left ventricle are expressed in molar. Data shown are from a single experiment ($n = 5$) and representative of three separate repeated experiments. *Error bars*, S.D.

Interestingly, if GAGs binding to VEGF$_{165}$, FGF-1, and FGF-2 were modified by the aging process, it was not the case for HB-EGF. This differential binding is in accord with the "multiple binding sites" theory describing the presence of "major" binding sites, which interact with several proteins, and "unique" or "modulating" binding sites, which interact more specifically with individual proteins to regulate particular biological processes (37). Our results suggest that these unique binding sites may exist and vary as a consequence of aging.

In addition to the fine structural alterations of HS in the aging myocardium, we observed some age-related changes in the HS spatial distribution, characterized by an increased deposition of aggregate-like spots. The presence of these aggregate-like corps

is of particular interest because they might have physiological significance. GAGs, and particularly HS, are known to be present in most amyloid protein aggregates and to play important roles on amyloid fibril formation, stability, and resistance to proteolysis (38). Cardiac protein aggregation has been associated with the aging process and suggested to play important roles in the development of heart diseases such as congestive heart failure (39, 40). The role of HS in cardiac protein aggregation as a consequence of aging should be further investigated.

Besides the effect of HS on growth factors activities, our study showed no differences in the chondroitin sulfate levels and FGF-2 binding capacities. This is in accord with previous studies showing that chondroitin sulfates fail to form a FGF-FGFR-chondroitin sulfate ternary complex (35). Thus, we suggest that chondroitin sulfate may not outstandingly contribute to the age-related GAGs functional changes observed in this work.

CONCLUSION

Taken together, our results show that HS are increased in myocardium left ventricle in aged subjects and that this increase is associated with changes in their capacities to differently interact and activate growth factors as VEGF, FGF-1, and FGF-2, known for their cardioprotective and cardioregulatory properties. To our knowledge, this is one of the first reports in nongenetically modified animals in which averred structural changes of endogenous HS directly correlates with the regulation of growth factor functionalities during a particular physiological event, here aging. Overall, the study demonstrates the importance of the HS structures on the control of key tissue repair effectors and suggests that the quality of HS could be associated with an age-dependent alteration of the ECM quality. This might affect tissue homeostasis and participate in heart function impairment in elderly, as illustrated by the decreased abilities of aged GAGs to bind and potentiate FGF-2 activity. However, this also suggests that some homeostasis regulatory mechanisms take place in the aging tissue to stimulate angiogenic factors as VEGF through modification of HS structural

features. Thus, based in the analysis of GAG structures and functionalities, one can conceive the possibility of designing a proper ECM environment for a suitable hosting of endogenous or therapeutic growth factors or colonizing cells, as stem cells or progenitors, to improve current tissue remodeling or repair strategies.

REFERENCES

1. Marastoni, S., Ligresti, G., Lorenzon, E., Colombatti, A., and Mongiat, M. (2008) Extracellular matrix: a matter of life and death. *Connect. Tissue Res.* **49,** 203–206
2. Najafi, F., Jamrozik, K., and Dobson, A. J. (2009) Understanding the "epidemic of heart failure": a systematic review of trends in determinants of heart failure. *Eur. J. Heart Fail.* **11,** 472–479
3. Yung, S., and Chan, T. M. (2007) Glycosaminoglycans and proteoglycans: overlooked entities? *Perit. Dial. Int.* **27,** S104–109
4. Ori, A., Wilkinson, M. C., and Fernig, D. G. (2008) The heparanome and regulation of cell function: structures, functions and challenges. *Front. Biosci.* **13,** 4309–4338
5. Sasisekharan, R., and Venkataraman, G. (2000) Heparin and heparan sulfate: biosynthesis, structure and function. *Curr. Opin. Chem. Biol.* **4,** 626–631
6. Zakrzewska, M., Marcinkowska, E., and Wiedlocha, A. (2008) FGF-1: from biology through engineering to potential medical applications. *Crit. Rev. Clin. Lab. Sci.* **45,** 91–135
7. Beenken, A., and Mohammadi, M. (2009) The FGF family: biology, pathophysiology and therapy. *Nat. Rev. Drug Discov.* **8,** 235–253
8. Kardami, E., Detillieux, K., Ma, X., Jiang, Z., Santiago, J. J., Jimenez, S. K., and Cattini, P. A. (2007) Fibroblast growth factor-2 and cardioprotection. *Heart Fail. Rev.* **12,** 267–277
9. Gaffney, M. M., Hynes, S. O., Barry, F., and O'Brien, T. (2007) Cardiovascular gene therapy: current status and therapeutic potential. *Br. J. Pharmacol.* **152,** 175–188
10. Lavu, M., Gundewar, S., and Lefer, D. J. (2011) Gene therapy for ischemic heart disease. *J. Mol. Cell Cardiol.* **50,** 742–750
11. Prokopi, M., and Mayr, M. (2011) The article is Proteomics: a reality-check for putative stem cells. *Circ. Res.* **108,** 499–511
12. Barbosa, I., Garcia, S., Barbier-Chassefière, V., Caruelle, J. P., Martelly, I., and Papy-García, D. (2003) Improved and simple micro assay for sulfated glycosaminoglycans quantification in biological extracts and its use in skin and muscle tissue studies. *Glycobiology* **13,** 647–653
13. Najjam, S., Gibbs, R. V., Gordon, M. Y., and Rider, C. C. (1997) The binding of interleukin 2 to heparin revealed by a novel ELISA method. *Biochem. Soc. Trans.* **25,** 3S
14. Ornitz, D. M., Yayon, A., Flanagan, J. G., Svahn, C. M., Levi, E., and Leder, P. (1992) Heparin is required for cell-free binding of basic fibroblast growth factor to a soluble receptor and for mitogenesis in whole cells. *Mol. Cell. Biol.* **12,** 240–247
15. Rouet, V., Hamma-Kourbali, Y., Petit, E., Panagopoulou, P., Katsoris, P., Barritault, D., Caruelle, J. P., and Courty, J. (2005) A synthetic glycosaminoglycan mimetic binds vascular endothelial growth factor and modulates angiogenesis. *J. Biol. Chem.* **280,** 32792–32800
16. Gillies, R. J., Didier, N., and Denton, M. (1986) Determination of cell number in monolayer cultures. *Anal. Biochem.* **159,** 109–113
17. Blondet, B., Carpentier, G., Lafdil, F., and Courty, J. (2005) Pleiotrophin cellular localization in nerve regeneration after peripheral nerve injury. *J. Histochem. Cytochem.* **53,** 971–977
18. Blondet, B., Carpentier, G., Ferry, A., and Courty, J. (2006) Exogenous pleiotrophin applied to lesioned nerve impairs muscle reinnervation. *Neurochem. Res.* **31,** 907–913
19. Toyoda, H., Yamamoto, H., Ogino, N., Toida, T., and Imanari, T. (1999) Rapid and sensitive analysis of disaccharides composition in heparin and heparan sulfate by reverse phase ion pair chromatography on a 2 mm porous silica gel column. *J. Chromatog. A* **830,** 197–201
20. Kurup, S., Wijnhoven, T. J., Jenniskens, G. J., Kimata, K., Habuchi, H., Li J. P., Lindahl, U., van Kuppevelt, T. H., and Spillmann, D. (2007) Characterization of anti-heparan sulfate phage display antibodies AO4B08 and HS4E4. *J. Biol. Chem.* **282,** 21032–21042
21. Wijnhoven, T. J., van de Westerlo, E. M., Smits, N. C., Lensen, J. F., Rops, A. L., van der Vlag, J., Berden, J. H., van den Heuvel, L. P., and van Kuppevelt, T. H. (2008) Characterization of anticoagulant heparinoids by immunoprofiling. *Glycoconj. J.* **25,** 177–185
22. Smits, N. C., Kurup, S., Rops, A. L., ten Dam, G. B., Massuger, L. F., Hafmans, T., Turnbull, J. E., Spillmann, D., Li J. P., Kennel, S. J., Wall, J. S., Shworak, N. W., Dekhuijzen, P. N., van der Vlag, J., and van Kuppevelt, T. H. (2010) The heparan sulfate motif (GlcNS6S-IdoA2S)3, common in heparin, has a strict topography and is involved in cell behavior and disease. *J. Biol. Chem.* **285,** 41143–41151
23. Lensen, J. F., Rops, A. L., Wijnhoven, T. J., Hafmans, T., Feitz, W. F., Oosterwijk, E., Banas, B., Bindels, R. J., van den Heuvel, L. P., van der Vlag, J., Berden, J. H., and van Kuppevelt, T. H. (2005) Localization and functional characterization of glycosaminoglycan domains in the normal human kidney as revealed by phage display-derived single chain antibodies. *J. Am. Soc. Nephrol.* **16,** 1279–1288
24. Wijnhoven, T. J., Lensen, J. F., Rops, A. L., van der Vlag, J., Kolset, S. O., Bangstad, H. J., Pfeffer, P., van den Hoven, M. J., Berden, J. H., van den Heuvel, L. P., and van Kuppevelt, T. H. (2006) Aberrant heparan sulfate profile in the human diabetic kidney offers new clues for therapeutic glycomimetics. *Am. J. Kidney Dis.* **48,** 250–261
25. Smits, N. C., Robbesom, A. A., Versteeg, E. M., van de Westerlo, E. M., Dekhuijzen, P. N., and van Kuppevelt, T. H. (2004) Heterogeneity of heparan sulfates in human lung. *Am. J. Respir. Cell Mol. Biol.* **30,** 166–173
26. Ten Dam, G. B., Kurup, S., van de Westerlo, E. M., Versteeg, E. M., Lindahl, U., Spillmann, D., and van Kuppevelt, T. H. (2006) 3-O-Sulfated oligosaccharide structures are recognized by anti-heparan sulfate antibody HS4C3. *J. Biol. Chem.* **281,** 4654–4662
27. Lensen, J. F., Wijnhoven, T. J., Kuik, L. H., Versteeg, E. M., Hafmans, T., Rops, A. L., Pavao, M. S., van der Vlag, J., van den Heuvel, L. P., Berden, J. H., and van Kuppevelt, T. H. (2006) Selection and characterization of a unique phage display-derived antibody against dermatan sulfate. *Matrix Biol.* **25,** 457–461
28. Smetsers, T. F., van de Westerlo, E. M., ten Dam G. B., Overes, I. M., Schalkwijk, J., van Muijen G. N., and van Kuppevelt, T. H. (2004) Human single-chain antibodies reactive with native chondroitin sulfate detect chondroitin sulfate alterations in melanoma and psoriasis. *J. Invest. Dermatol.* **122,** 707–716
29. Ten Dam, G. B., Yamada, S., Kobayashi, F., Purushothaman, A., van de Westerlo, E. M., Bulten, J., Malmström, A., Sugahara, K., Massuger, L. F., and van Kuppevelt, T. H. (2009) Dermatan sulfate domains defined by the novel antibody GD3A12, in normal tissues and ovarian adenocarcinomas. *Histochem. Cell Biol.* **132,** 117–127
30. Purushothaman, A., Fukuda, J., Mizumoto, S., ten Dam, G. B., van Kuppevelt, T. H., Kitagawa, H., Mikami, T., and Sugahara, K. (2007) Functions of chondroitin sulfate/dermatan sulfate chains in brain development: critical roles of E and iE disaccharide units recognized by a single chain antibody GD3G7. *J. Biol. Chem.* **282,** 19442–19452
31. Deschamps, A. M., and Spinale, F. G. (2005) Matrix modulation and heart failure: new concepts question old beliefs. *Curr. Opin. Cardiol.* **20,** 211–216
32. Narita, K., Staub, J., Chien, J., Meyer, K., Bauer, M., Friedl, A., Ramakrishnan, S., and Shridhar, V. (2006) HSulf-1 inhibits angiogenesis and tumorigenesis *in vivo*. *Cancer Res.* **66,** 6025–6032
33. Frese, M. A., Milz, F., Dick, M., Lamanna, W. C., and Dierks, T. (2009) Characterization of the human sulfatase Sulf1 and its high affinity heparin/heparan sulfate interaction domain. *J. Biol. Chem.* **284,** 28033–28044
34. Stringer, S. E. (2006) The role of heparan sulphate proteoglycans in angiogenesis. *Biochem. Soc. Trans.* **34,** 451–453
35. Zhang, X., Ibrahimi, O. A., Olsen, S. K., Umemori, H., Mohammadi, M.,

and Ornitz, D. M. (2006) Receptor specificity of the fibroblast growth factor family: the complete mammalian FGF family. *J. Biol. Chem.* **281,** 15694–15700

36. Ashikari-Hada, S., Habuchi, H., Sugaya, N., Kobayashi, T., and Kimata, K. (2009) Specific inhibition of FGF-2 signaling with 2-*O*-sulfated octasaccharides of heparan sulfate. *Glycobiology* **19,** 644–654

37. Chu, C. L., Goerges, A. L., and Nugent, M. A. (2005) Identification of common and specific growth factor binding sites in heparan sulfate proteoglycans. *Biochemistry* **44,** 12203–12213

38. Naiki, H., and Nagai, Y. (2009) Molecular pathogenesis of protein misfolding diseases: pathological molecular environments *versus* quality control systems against misfolded proteins. *J. Biochem.* **146,** 751–756

39. Wang, X., Su, H., and Ranek, M. J. (2008) Protein quality control and degradation in cardiomyocytes. *J. Mol. Cell. Cardiol.* **45,** 11–27

40. Wang, X., and Robbins, J. (2006) Heart failure and protein quality control. *Circ. Res.* **99,** 1315–1328